Synthetic Inhibitors of Cytochrome P-450 2A6: Inhibitory Activity, Difference Spectra, Mechanism of Inhibition, and Protein Cocrystallization

Jason K. Yano,[†,‡] Travis T. Denton,[§,‡] Matthew A. Cerny,[§] Xiaodong Zhang,[§] Eric F. Johnson,[†] and John R. Cashman*,[§]

Human BioMolecular Research Institute, 5310 Eastgate Mall, San Diego, California 92121, and Molecular and Experimental Medicine, MEM-255, The Scripps Research Institute, La Jolla, California 92037

A series of 3-heteroaromatic analogues of nicotine were synthesized to delineate structural and mechanistic requirements for selectively inhibiting human cytochrome P450 (CYP) 2A6. Thiophene, substituted thiophene, furan, substituted furan, acetylene, imidazole, substituted imidazole, thiazole, pyrazole, substituted pyrazole, and aliphatic and isoxazol moieties were used to replace the *N*-methylpyrrolidine ring of nicotine. A number of potent inhibitors were identified, and several exhibited high selectivity for CYP2A6 relative to CYP2E1, -3A4, -2B6, -2C9, -2C19, and -2D6. The majority of these inhibitors elicited type II difference spectra indicating the formation of a coordinate covalent bond to the heme iron. The majority of inhibitors were reversible inhibitors although several mechanism-based inactivators were identified. Most of the inhibitors were also relatively metabolically stable. X-ray crystal structures of CYP2A6 cocrystallized with three furan analogues bearing methanamino side chains indicated that the amine side chain coordinated to the heme iron. The pyridyl moiety was positioned to accept a hydrogen bond from Asn297, and all three inhibitors exhibited orthogonal aromatic−aromatic interactions with protein side chains. For comparison, the cocrystal structure of 4,4′-dipyridyl disulfide was also obtained and showed that the pyridine moiety could assume a different orientation than that observed for the 3-heteroaromatic pyridines examined. For the 3-heteroromatic pyridines, *N*-methyl and *N,N*-dimethyl amino groups increased the apparent K_i and distorted helix I of the protein. Substitution of a phenyl ring for the pyridyl ring also increased the apparent K_i, which is likely to reflect the loss of the hydrogen bonding interaction with Asn297. In contrast, inhibitory potency for other P450s was increased, and the selectivity of the phenyl analogues for CYP2A6 was decreased relative to the pyridyl compounds. The results suggest that inhibitors that compliment the active site features of CYP2A6 can exhibit significant selectivity for CYP2A6 relative to other human liver drug-metabolizing P450s.

Introduction

In the United States, active smoking is the leading cause of preventable disease, disability, and death.[1] Smoking is also the causative factor in 80−90% of lung cancer cases estimated to claim over 440 000 lives in the United States during 2005 and an additional 50 000 excess deaths from exposure to secondhand smoke.[1] Despite the widespread knowledge of the health-related consequences associated with cigarette smoking, millions of people nationwide continue to smoke though many desire to stop. Cessation of smoking has been shown to have immediate health benefits even to long-term smokers.[2] Approximately 35% of smokers attempt to quit each year, but only 5% are successful.[3]

Currently, few pharmacotherapies exist for smoking cessation. The most widely used therapies include (1) nicotine replacement therapies (NRT) in the form of inhalers, patches, nasal spray, and gum, (2) the dopamine reuptake inhibitor bupropion, (3) the tricyclic antidepressant nortryptaline, and (4) the antianxiety agent buspirone. Common to each of these therapies are use-limiting side effects and success rates typically below 40%.[3,4] These factors suggest that implementation of new smoking cessation agents with novel mechanisms of action is warranted.

Recent work has focused on inhibition of the cytochrome P450 enzyme (CYP) involved in nicotine metabolism as a means of smoking cessation. CYP2A6 is found predominantly in the liver where it accounts for approximately 1−10% of total CYP content.[5] However, this enzyme is responsible for 70−80% of the initial metabolism of nicotine[6] via the intermediacy of the aldehyde oxidase-catalyzed iminium ion that is converted to the major excreted and nonpsychoactive metabolite, cotinine.[7] For this reason, CYP2A6 has been proposed to be a novel target for smoking cessation. Inhibition of CYP2A6 has been shown to result in altered pharmacokinetics for nicotine resulting in an increased plasma half-life.[8] Inhibition of nicotine metabolism should result in a diminished desire to smoke and a lessening of the ingestion of toxic or carcinogenic components of cigarette smoke, and some evidence in support of this point has been reported.[8] CYP2A6 inhibitors may aid in the cessation of smoking.[9]

Although a number of compounds have been used as inhibitors of CYP2A6 including tranylcypromine and methoxsalen, these compounds generally lack selectivity for targeting CYP2A6 and may also inhibit other drug-metabolizing enzymes and therefore could result in untoward drug−drug interactions.[10] On the basis of nicotine as a lead structure, we have previously described a number of CYP2A6 inhibitors of which several show considerable selectivity for CYP2A6 versus other drug-metabolizing CYPs.[11] In this report, we describe the synthesis and testing of several new 3-heteroaromatic and 3-aliphatic pyridine analogues and also include microsomal stability data for these compounds. We show that some of the most potent compounds are also mechanism-based inactivators of CYP2A6. Furthermore, we have also obtained cocrystal structures of CYP2A6 with some of these inhibitors including a series of

---

* To whom correspondence should be addressed. Tel: 858-458-9305. Fax: 858-458-9311. E-mail: jcashman@hbri.org.
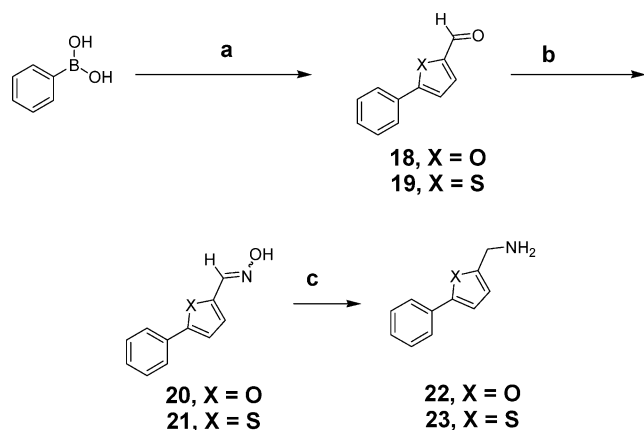† The Scripps Research Institute.
‡ J.K.Y. and T.T.D. contributed equally to this work.
§ Human BioMolecular Research Institute.

Scheme 1. Synthesis of Sulfur-Containing (Furan-2-yl)pyridines[a]
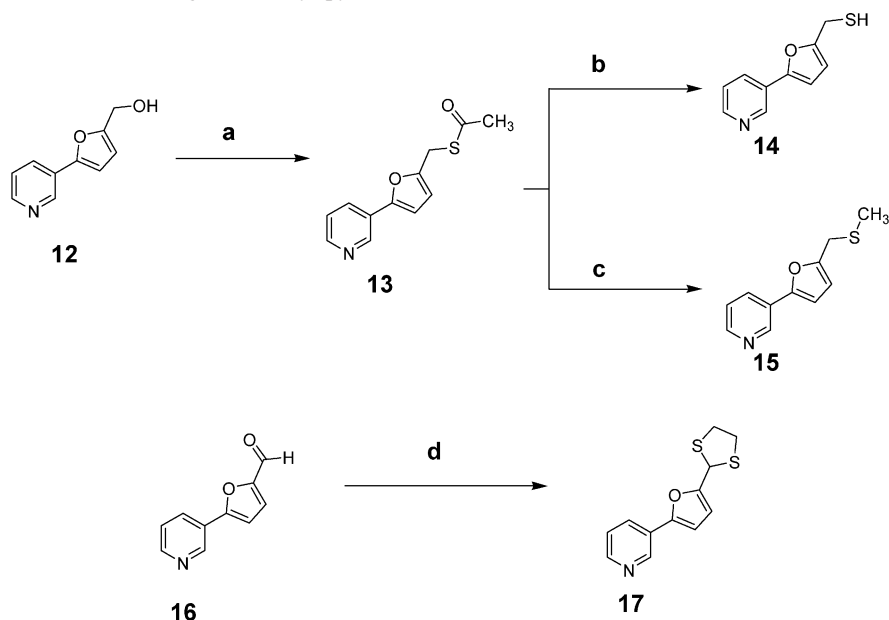
[a] (a) PBr$_3$, potassium thioacetate; (b) NaSCH$_3$; (c) NaOCH$_3$, CH$_3$I; (d) ethane thiol, toluene sulfonic acid.

Scheme 2. Synthesis of (5-Phenyl heteroaromatic) Methanamines[a]

[a] (a) Heteroaryl bromide, Pd(PPh$_3$)$_4$, Na$_2$CO$_3$; (b) NH$_2$OH, HCl, NaOAc; (c) LAH, THF.

3-heteroaromatic pyridines related to nicotine possessing primary, secondary, or tertiary amino groups. In addition, we determined the cocrystal structure of 4,4′-dipyridyl disulfide, a known inhibitor of CYP2A6. The mechanism data and cocrystal structures offer interesting insights into inhibitor binding and also provide considerable information for further inhibitor design.

Results and Discussion

Inhibition of recombinant human CYP2A6 as assessed by the functional activity of coumarin 7-hydroxylation was characterized. The mechanism of CYP2A6 inhibition was examined in detail by determining the time-dependent nature of the inhibition and the spectral binding properties of 30 compounds. The metabolic stability in the presence of mouse and human liver microsomes was investigated, and the selectivity of inhibition was examined for CYP2A6, -3A4, -2E1, -2B6, -2C9, -2C19, and -2D6. To examine the interaction of selected inhibitors in detail, cocrystallization with CYP2A6 was accomplished. The results provided a comprehensive picture of the inhibition of CYP2A6 in the presence of 3-heteroaromatic pyridine analogues of nicotine.

Scheme 3. Synthesis of 3-phenylthiophenes[a]
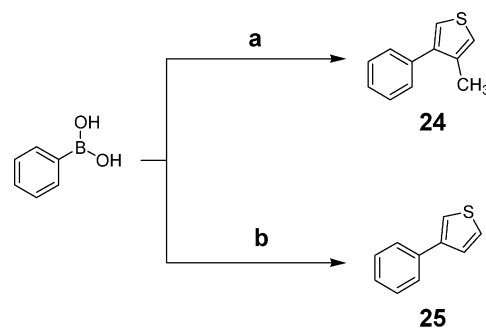
[a] (a) 3-methyl 4-bromothiophene, Pd(PPh$_3$)$_4$, Na$_2$CO$_3$; (b) 3-bromothiophene, Pd(PPh$_3$)$_4$, Na$_2$CO$_3$.

The target compounds were efficiently synthesized and characterized by procedures previously described (Schemes 1−5).[11] HPLC-based analytical methods (Supporting Information) and biochemical assays were used to assess the metabolic stability of compounds **1**−**35** in the presence of mouse and human liver microsomes. This was done to ascertain the stability of the compounds toward oxidative metabolism in advance of more detailed studies with highly purified CYPs, as well as to determine whether the inhibitors were operating as time-dependent inhibitors. In general, the majority of compounds **1**−**35** were metabolically quite stable (Table 1). With the exception of compounds **2a**, **4**, **11**, **13**, **22**, and **26**, most of the compounds possessed half-life values in excess of 40 min. Generally, compounds that were rapidly metabolized by mouse liver microsomes were also rapidly metabolized by human liver microsomes. However, compounds **1a**, **16**, and **24** were possible exceptions to this general observation. Overall, we interpret this to suggest that the mouse and human liver CYP2A enzymes are quite similar and are inhibited in a common manner and by the same mechanism. This is in agreement with previous studies that have shown that mouse CYP2A5 is 94% similar to the human CYP2A6 amino acid sequence.[12] Generally, compounds that were metabolically stable in the presence of mouse or human liver microsomal preparations did not afford evidence of significant amounts of metabolite formation (Table 1).

Scheme 4. Synthesis of 3-Substituted Pyridines[a]
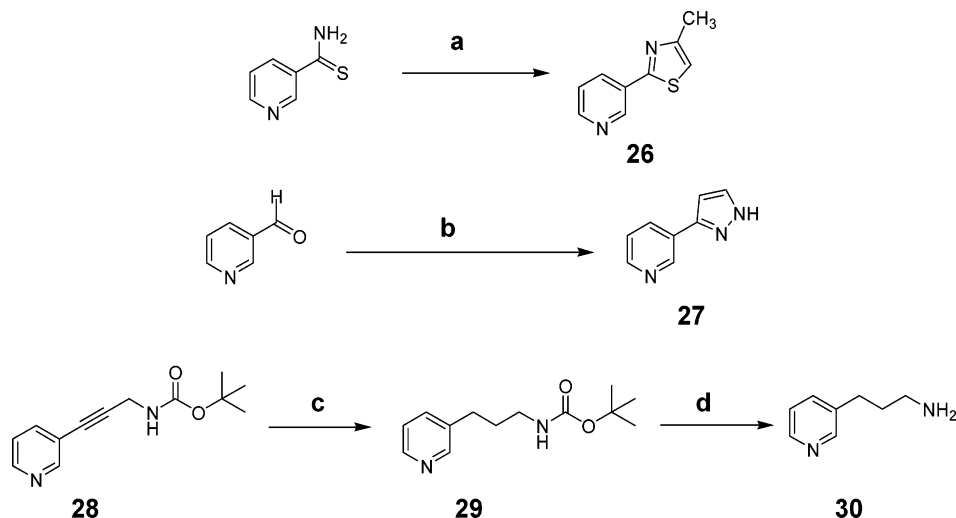
[a] (a) Chloroacetone, ΔH; (b) 2-tosylhydrazine, 1-vinyl imidazole; (c) H$_2$/10% PdC; (d) TFA/CH$_2$Cl$_2$.

Scheme 5. Synthesis of Pyrazol- and Isoxazol Pyridine Derivatives[a]
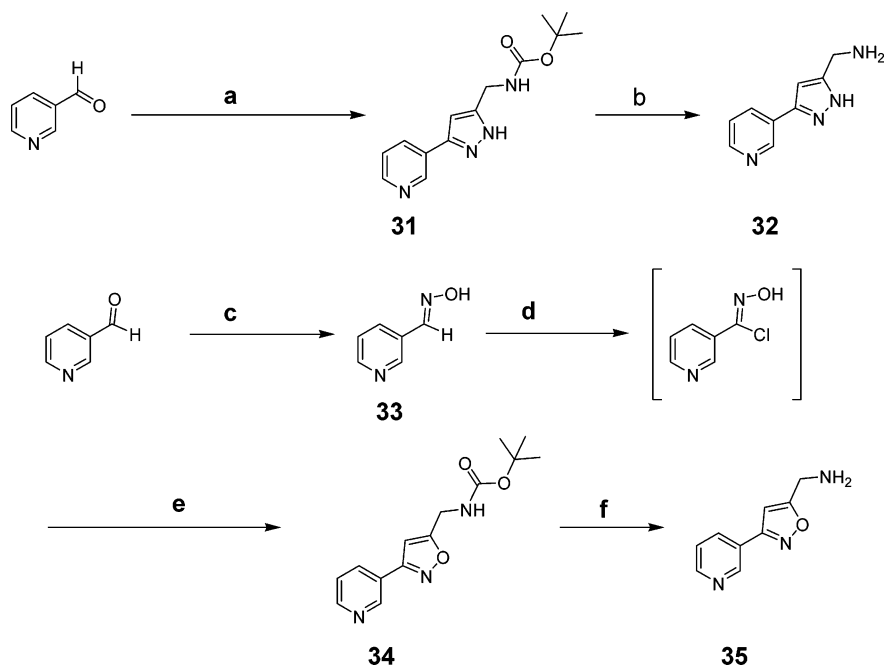
[a] (a) 2-Tosylhydrazine, NaOH, *tert*-butyl prop-2-ynyl carbamate; (b) TFA/CH$_2$Cl$_2$; (c) NH$_2$OH, HCl, NaOAc; (d) *N*-chlorosuccinimide/DMF; (e) *tert*-butyl prop-2-ynyl carbamate, Et$_3$N; (f) HCl/1,4-dioxane.

Possible exceptions to this observation were seen for some thiophene-containing inhibitors (i.e., **1a**, **4**, **8**, and **11**), which appeared to be oxidized in the presence of mouse and human liver microsomes. It is possible that the thiophene compounds were oxidized by CYP2A6 or non-CYP2A6 enzymes as has been described previously for other thiophene-containing compounds.[13] In addition to the substituted thiophene compounds examined, two furan-containing compounds (i.e., **2a** and **2b**) appeared to be oxidized in the presence of human liver microsomes. Metabolic oxidation of thiophenes and furans can lead to reactive metabolites and CYP inhibition.[14]

Time-Dependent Inhibitors. The compounds shown in Table 1 were also screened to identify potential time-dependent inhibitors at a concentration 10-fold the K_i value. Sulfur-containing compounds **4**, **13**, **14**, and **17** afforded time-dependent inhibition of CYP2A6 with half-lives of 12.3, 3.0, 13.7, and 41.3 min, respectively. Compounds **14** and **15** were equipotent inhibitors of CYP2A6 (Table 2), but **17** was considerably less

potent. This suggests that some room was available in the CYP2A6 active site proximal to the heme but larger substituents introduced steric interference. Because **15** did not show time-dependent inactivation of CYP2A6 and **13** was judged hydrolytically unstable, they were not studied further. Compounds **4** and **14** showed time-dependent inhibition of CYP2A6 at the initial $10 \times K_i$ concentration, and they were chosen for full kinetic characterization. Four concentrations (i.e., 0.7-, 1-, 2-, and 10-fold the K_i value) were used to determine the time-dependent kinetic parameters for the selected compounds, and they afforded linear plots of the log of the remaining CYP2A6 enzyme activity versus time. A replot of the kinetic data in reciprocal form (i.e., $1/k$ versus $1/[I]$) gave linear plots ($r^2 = 0.999$). Compound **4** was determined to be a time-dependent inactivator with a $k_{inactivation}$ value of 0.02 min^{-1}. Similarly, compound **14** was examined kinetically and was also found to be a time-dependent inactivator with a $k_{inactivation}$ value of 0.04 min^{-1}.

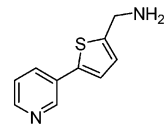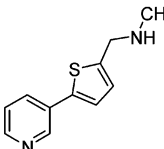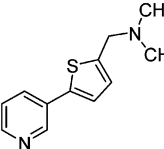**Table 1.** Metabolic Stability, Binding Type, and Metabolites of CYP2A6 Inhibitors
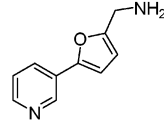
Compd	Structure	Binding Type	MLM[a] $t_{1/2}$	Major MLM Metabolite	HLM[a] $t_{1/2}$	Major HLM Metabolite
		min/max	(min)		(min)	
1a		Type II 409/428	60	$[M-NH_2]^+ + 18$	39	$[M-NH_2]^+ + 18$
1b		Type II 410/430	Stable[a]	No Products Observed	96	No Products Observed
1c		Type II 411/428	343	No Products Observed	Stable[a]	No Products Observed
2a		Type II 409/428	37	No Products Observed	37	$[M-NH_2]^+ + 18$
2b		Type II 411/431	Stable[a]	No Products Observed	66	$[M-NH(CH_3)]^+ + 18$
2c		Type II 411/430	Stable[a]	No Products Observed	331	No Products Observed
3a		Type II 410/430	74	No Products Observed	63	No Products Observed
3b		Type II 410/428	123	No Products Observed	136	No Products Observed
3c		No Shift[a]	Stable[a]	No Products Observed	Stable[a]	No Products Observed
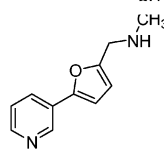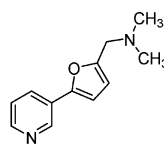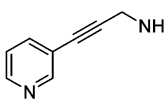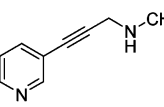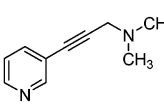
Table 1 (Continued)

Compd	Structure	Binding Type min/max	MLM[a] $t_{1/2}$ (min)	Major MLM Metabolite	HLM[a] $t_{1/2}$ (min)	Major HLM Metabolite
4		Type I 414/383	41	$[M+H]^{+}+16$	32	$[M+H]^{+}+16$
5		Type II 409/429	481	No Products Observed	Stable[a]	No Products Observed
6		Type II 410/428	Stable[a]	No Products Observed	118	No Products Observed
7		Type I 418/385	Stable[a]	No Products Observed	84	No Products Observed
8		Type II 409/427	Stable[a]	$[M+H]^{+}\textbf{+16}$	271	No Products Observed
9		Type II 409/428	Stable[a]	No Products Observed	133	No Products Observed
10		Type II 410/427	698	No Products Observed	701	No Products Observed
11		Type II 410/427	47	$[M+H]^{+}+16$	32	$[M+H]^{+}+16$
13		No Shift (Coumarin (-)[b]	18	ND	30	ND
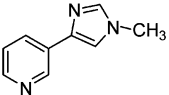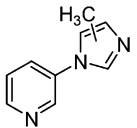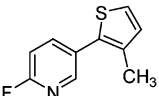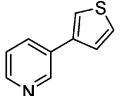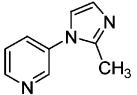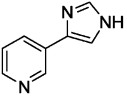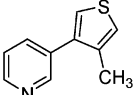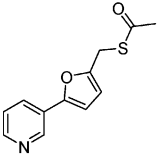
Table 1 (Continued)

Compd	Structure	Binding Type min/max	MLM[a] t$_{1/2}$ (min)	Major MLM Metabolite	HLM[a] t$_{1/2}$ (min)	Major HLM Metabolite
14		No Shift (Coumarin (+)[c]	105	ND	119	ND
15		Type II 410/431	38	ND	59	ND
17		No Shift (Coumarin (+)[c]	24	ND	92	ND
22		Type II 410/430	22	ND	37	ND
23		Type II 410/431	41	No Products Observed	84	No Products Observed
24		Type I 416/385	37	ND	74	ND
25		Type I 416/385	92	No Products Observed	315	No Products Observed
26		Type I 416/385	49	ND	36	ND
27		Type II 410/427	93	No Products Observed	99	No Products Observed
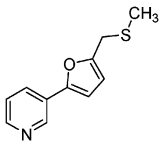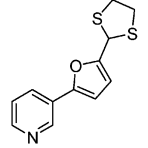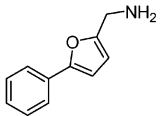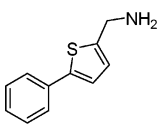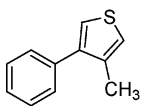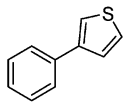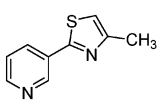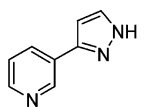
Table 1 (Continued)

Compd	Structure	Binding Type min/max	MLM[a] $t_{1/2}$ (min)	Major MLM Metabolite	HLM[a] $t_{1/2}$ (min)	Major HLM Metabolite
30		Type II 410/430	Stable	No Products Observed	Stable	No Products Observed
32		Type II 410/430	169	No Products Observed	238	No Products Observed
35		Type II 410/430	385	No Products Observed	401	No Products Observed
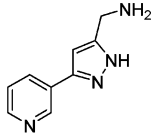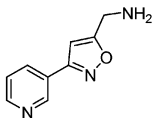
[a] During the mouse liver (MLM) or human liver microsome (HLM) incubations, no detectable loss of parent compound was observed. [b] The P4502A6dH protein was preincubated with coumarin (2.5 μM), a type I spectral shift was recorded, and the test compound (100 μM) was added and, due to the low potency of the compound, failed to completely displace coumarin. [c] The P4502A6dH protein was preincubated with coumarin (2.5 μM), a type I spectral shift was recorded, and the test compound (100 μM) was added and completely displaced coumarin.

Table 2. Inhibition of CYP2A6, CYP3A4, CYP2E1, CYP2B6, CYP2C9, CYP2C19, and CYP2D6 by Synthetic 3-Heteroaromatic Pyridine Analogues of Nicotine

compd	$K_i \pm$ SD (μM)						
	2A6	3A4	2E1	2B6	2C9	2C19	2D6
1a	0.08 ± 0	29.4 ± 8	20.1 ± 9	26.1 ± 4	4.5 ± 0.7	1.0 ± 0.1	84.5 ± 9
1b	0.6 ± 0.1	$>400^a$	$>400^a$	$>400^a$	33.9 ± 2	29.9 ± 3	56.5 ± 10
1c	66.5 ± 11	110 ± 12	$>400^a$	$>400^a$	103 ± 12	53 ± 9	14.4 ± 2.1
2a	$0.1 \pm 0.$	23.6 ± 9	86 ± 26	95.5 ± 12	5.9 ± 1.1	11 ± 0.8	5.7 ± 1.3
2b	0.8 ± 0.2	$>400^a$	$>400^a$	179 ± 11	38.1 ± 5	15.3 ± 2	45.3 ± 4
2c	14.2 ± 9	147 ± 13	$>400^a$	$>400^a$	111 ± 8	79 ± 5	127 ± 18
3a	0.3 ± 0	15.2 ± 4	10.5 ± 3	82.5 ± 23	1.2 ± 0.2	12.9 ± 2	60.5 ± 23
3b	2.7 ± 0.3	251 ± 52	117 ± 25	60 ± 18	6.3 ± 1	16.4 ± 3	$>400^a$
3c	67.5 ± 24	$>400^a$	$>400^a$	192 ± 23	$>400^a$	$>400^a$	$>400^a$
4	0.3 ± 0.1	3.0 ± 0.6	3.5 ± 1.0	1.9 ± 0.4	46.6 ± 4	10.1 ± 10	48 ± 1
5	0.4 ± 0.1	131 ± 32	2.0 ± 0.4	73 ± 10	39.7 ± 5	61 ± 6	102 ± 11
6	0.5 ± 0.1	54.5 ± 23	29 ± 6	$>300^a$	$>300^a$	$>300^a$	149 ± 15
7	0.6 ± 0.1	$19.6 \pm 6.$	184 ± 40	5.9 ± 1	$>400^a$	21 ± 1	$>400^a$
8	0.7 ± 0.1	28 ± 10	$>400^a$	30 ± 2	48.2 ± 5	55.6 ± 3	124 ± 18
9	0.7 ± 0.2	76 ± 35	54.5 ± 6	$>300^a$	$>300^a$	$>300^a$	$>300^a$
10	0.8 ± 0.2	70 ± 7	12.8 ± 2	$51.5 \pm .5$	20.9 ± 3	26.8 ± 2	100 ± 22
11	0.9 ± 0.3	$<25^b$	3.1 ± 1	3.1 ± 0.3	61.5 ± 6	12.5 ± 1	96.5 ± 14
13	0.8 ± 0.2	1.5 ± 0.8	$0.2 \pm 0.$	0.9 ± 0.2	2.9 ± 0.6	3.9 ± 0.4	45.4 ± 9
14	$<0.8^b$	3.1 ± 2^c	0.05 ± 0	1.1 ± 0.3	0.4 ± 0.1	0.2 ± 0	0.7 ± 0.1
15	0.8 ± 0.1	7.4 ± 1	0.8 ± 0.1	46.9 ± 8	14.1 ± 3	7.0 ± 0.6	64.5 ± 10
17	13.9 ± 3.3	1.1 ± 0.6	0.6 ± 0.1	5.3 ± 0.7	1.3 ± 0.2	0.7 ± 0.1	38.4 ± 4
22	0.6 ± 0.1	63 ± 14	0.8 ± 0.2	3.8 ± 1	0.9 ± 0.2	41 ± 0.9	$14.8 \pm 4.$
23	0.6 ± 0.1	95.5 ± 21	0.04 ± 0	0.6 ± 0.1	0.5 ± 0.1	0.9 ± 0.1	$>400^a$
24	6.2 ± 1	$>400^a$	$>400^a$	5.1 ± 0.9	$>400^a$	$>400^a$	$>400^a$
25	3.3 ± 0.3	$>400^a$	9.7 ± 3	14 ± 3	112 ± 20	107 ± 18	$>400^a$
26	4.1 ± 0.8	22.9 ± 4	9.6 ± 3	43.5 ± 10	51.5 ± 8	$>400^a$	$>400^a$
27	12.8 ± 1	$>400^a$	5.2 ± 1	71.5 ± 23	172 ± 30	109 ± 13	165 ± 35
30	6.6 ± 0.6	$>400^a$	$>400^a$	$>400^a$	$>400^a$	$>400^a$	$>400^a$
32	0.3 ± 0	$>400^a$	$>400^a$	33.2 ± 8	24.2 ± 5	41.4 ± 13	29.8 ± 10
35	0.4 ± 0.1	$>400^a$	38.9 ± 2	33.7 ± 5	14.5 ± 3	27.5 ± 5	$>400^a$

[a] No detectable inhibition was seen at the highest concentration tested. [b] The test compound was highly fluorescent, and an accurate value was not determined. [c] The test compound was highly fluorescent, and this gave rise to a high standard deviation.

Compounds **4** and **14** likely inactivated CYP2A6 by distinct mechanisms. It may be that the thiophene sulfur of **4** directly ligates to the heme iron, undergoes oxidation to a reactive sulfoxide that inactivates the enzyme, or both. The thiol sulfur atom of compound **14** may undergo oxidation to the sulfenic acid that inhibits the enzyme. We did not observe formation of the sulfenic acid, but it is likely to be unstable and to be rapidly converted to the disulfide although analysis of formation of the

Table 3. Selectivity Ratio $(K_i(CYPX)/K_i(CYP2A6))^a$ of 3-Heteroaromatic Pyridine Analogues of Nicotine for Inhibition of Human CYP3A4, -2E1, -2B6, -2C9, and -2C19 versus Human CYP2A6[b]

compd	3A4/2A6	2E1/2A6	2B6/2A6	2C9/2A6	2C19/2A6	2D6/2A6
1a	**345**	**236**	**307**	**52**	**12**	**994**
1b	**>364**	**>364**	**>364**	**62**	**54**	**103**
1c	1.6	>3	>3	1.5	0.8	0.2
2a	**174**	**637**	**707**	**43**	**81**	**42**
2b	**>250**	**>250**	**224**	**48**	**19**	**57**
2c	10	>14	>14	7.8	5.5	8.9
3a	59.6	41.2	324	4.7	50.8	237
3b	92.8	43.1	22.2	2.3	6.1	>74
3c	>3	>3	2.8	>3	>3	>3
4	10	11	6.3	150	39	155
5	**349**	**5**	**195**	**106**	**163**	**272**
6	109	58	>300	>300	>300	>300
7	5.9	285	9.1	>310	32	>310
8	40	>286	42	69	81	>286
9	101	73	>200	260	>200	>200
10	93	17	69	28	35	133
11	53	<14	3.4	66	14	104
13	1.7	0.3	1	3.4	4.6	53
14	>4.1	<0.1	>1.5	<0.5	<0.3	<0.9
15	9.2	0.9	59	18	8.8	81
17	0.1	0.04	0.4	0.1	0.1	2.8
22	105	1.3	6.4	1.5	6.8	24.6
23	159	0.1	1.1	0.8	1.4	>333
24	>400	2.9	4.2	33.9	32.3	60.6
25	>32.3	>32.3	0.8	>32.3	>32.3	>32.3
26	5.6	2.3	10.6	12.6	>32.3	>32.3
27	>15.6	0.4	5.6	13.4	8.5	12.9
30	>400	>30	>30	>30	>30	>30
32	**>690**	**>690**	**114**	**83.4**	**143**	**103**
35	**>541**	**105**	**91.1**	**39.1**	**74.3**	**>541**

[a] CYPX (as indicated)/CYP2A6. [b] Selected values were made bold to highlight the CYP2A6 inhibition selectivity.

disulfide was not undertaken. The lack of a spectral change upon addition of **14** to CYP2A6 does not support a mechanism involving direct ligation (Table 1). Despite the enhanced nucleophilicity of **14**, it is almost 6-fold less potent an inhibitor of CYP2A6 than **2a**. It is possible that the larger sulfur atom changes the interaction for both heme ligation and position of the distal pyridine ring nitrogen to accept a hydrogen bond with Asn297. On the other hand, shorter inhibitors such as **8** that lack a side chain nucleophile may trigger distortion in the interaction of the five-membered ring and the protein. It may be that for some inhibitors, the pyridine reorients to ligate to the heme iron. These points are considered in greater detail below.

As reported previously, thiophene- and furan-linked methylamines such as **1a** and **2a** (Table 2) were among the most potent and selective (Table 3) CYP2A6 inhibitors previously identified.[11] To examine the influence of addition of steric bulk on the amine functionality, the secondary and tertiary amines were synthesized and tested. For compounds with 3-methylamine substituents (i.e., **1a**–**1c**, **2a**–**2c**, and **3a**–**3c**), generally, addition of *N*-methyl groups increased the metabolic stability and decreased the amount of microsomal oxidation. *N*-Methyl substitution of the primary amine of compounds **1a**, **2a**, and **3a** to afford the tertiary amine also dramatically increased the K_i value for inhibition of CYP2A6. A similar observation was made for the thiol-containing inhibitor, compound **14**. Addition of a methyl group to the thiol **14** afforded compound **15**, which had decreased inhibitor potency and abrogated time-dependent CYP2A6 inhibition. Compound **15** also exhibited a type II spectral change, Table 1, suggesting that methylation of the thiol changed the orientation of **15** relative to the heme when compared with **14**. Based on mass spectral studies of the metabolites of the N-substituted amines, it did not appear that

Table 4. Data Collection and Refinement Statistics

ligand	4,4'-dipyridyl disulfide	2a	2b	2c
PDB identifier	2FDY	2FDW	2FDV	2FDU
resolution range (Å)	50.0−1.95	50.0−2.05	50.0−1.65	50.0−1.85
unique reflns	160 717	131 309	248 540	182 306
avg redundancy[a]	3.4 (2.6)	3.6 (3.6)	3.5 (2.6)	3.3 (2.2)
completeness (%)[a]	98.7 (91.3)	93.9 (99.9)	92.5 (84.3)	95.1 (70.4)
$(I/\sigma_{avg}I)^a$	7.6 (2.0)	16.4 (2.1)	28.5 (2.2)	13.4 (1.7)
$R_{symm}(I)^a$	0.089 (0.45)	0.09 (0.67)	0.037 (0.41)	0.038 (0.42)
R $(R_{free})^b$	0.21 (0.25)	0.21 (0.22)	0.19 (0.22)	0.19 (0.22)
RMSD bonds (Å)	0.006	0.006	0.023	0.020
RMSD angles (deg)	1.26	1.23	1.95	1.76

[a] Values are for the highest resolution shell. All data presented in the table was collected at the Stanford Synchrotron Radiation Laboratory on beamline 9-1. [b] The text set represented 5% of the unique reflections.

metabolic oxidation was occurring on the nitrogen atom, but further studies must be done to obviate this point (Table 1). Overall, studies of the modification of side chain amines or thiols suggest that the most potent inhibitors were the ones that possessed the most unencumbered nucleophilic moiety, but as described below, a hydrogen bond with Asn297 is also an important determinant of inhibitory potency of CYP2A6.

UV−visible spectroscopic data, Table 1, indicated that the three 3-heteroaromatic pyridine analogues of nicotine bound to the enzyme through coordination of a polar atom to the heme iron, most likely one of the two nitrogen atoms of the pyridine and amine moieties. Unfortunately, UV−visible spectroscopy data alone cannot distinguish which of the two nitrogen atoms coordinated to the heme iron. To identify the mode of binding and to better understand inhibitor interactions with the enzyme, the three amine analogues **2a**, **2b**, and **2c** were cocrystallized with the enzyme, and their structures were determined by X-ray crystallography. 4,4'-Dipyridyl disulfide, a potent inhibitor of CYP2A6, was also included in this study for comparison.[16] UV−visible spectroscopy indicated that 4,4'-dipyridyl disulfide also likely coordinated to the heme iron through one of the pyridyl nitrogens (data not shown). As described below, 4,4'-dipyridyl disulfide binding caused a distortion of the CYP2A6 protein.

Cocrystallization Studies. The enzyme inhibitor complexes were crystallized using conditions similar to those employed previously for CYP2A6dH complexed with the substrate coumarin bound in the active site.[15] The data used for structure determination were collected from single crystals that diffracted to limiting resolutions of 2.05, 1.65, 1.85, and 1.95 Å in the $P2_1$ space group for each of the **2a**, **2b**, **2c**, and 4,4'-dipyridyl disulfide complexes, respectively (Table 4). Isomorphous replacement using the structure of CYP2A6dH (PDB 1Z10) determined previously[15] was used for initial phasing of the data, followed by rounds of fitting and refinement. The position and orientation of each inhibitor in the active site was clearly defined in sigma A weighted electron density maps. The results indicated that all three 3-heteroaromatic pyridine analogues of nicotine (i.e., **2a**, **2b**, **2c**) coordinated to the heme iron through the nitrogen atom of the primary, secondary, or tertiary amino group, respectively (Figure 1). In each case, the nitrogen of the amino group was located directly above the heme iron in the axial ligation position at distances of 2.27 ± 0.02, 2.18 ± 0.03, or 2.38 ± 0.03 Å for the primary, secondary, or tertiary amine,
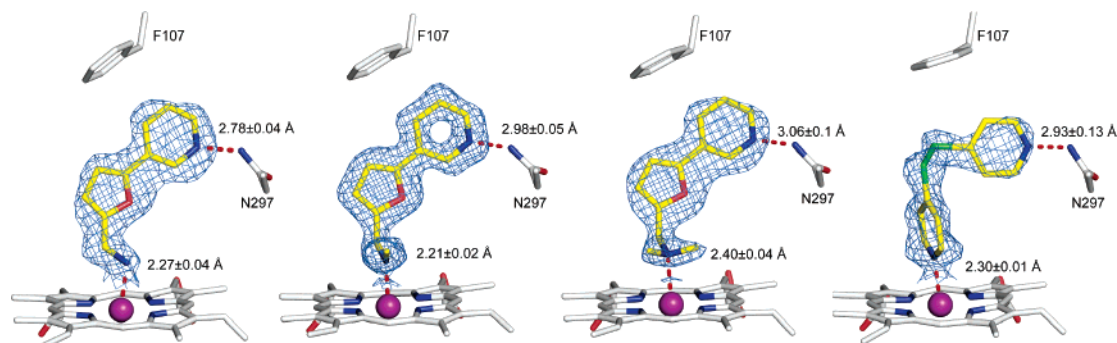
Figure 1. σA weighted $2|F_o| - |F_c|$ omit electron density maps contoured at 1 σ and rendered within 1.5 Å of the ligand for the complexes of CYP2A6 with **2a**, **2b**, **2c**, or 4,4′dipyridyl disulfide (left to right) bound in the active site. In each case, the substrate was omitted from the model used for the generation of the map. Carbon atoms are displayed in yellow for ligand or gray for the heme or protein, nitrogen atoms are in blue, oxygen atoms are in red, and the iron atom is in magenta. The dotted red lines indicate the potential for hydrogen bonding interactions with N297 or distance from the coordinating nitrogen to the heme iron.
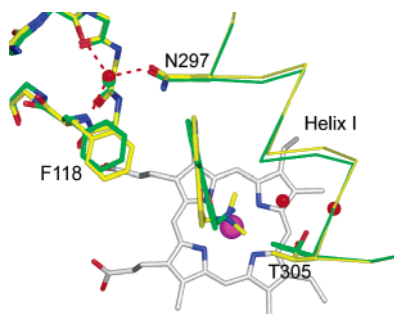

Figure 2. Cα-trace of helix I for the complexes of **2b** and **2c** bound in the active site of CYP2A6. The binding of the water molecules (red spheres) stabilizes distortions in the hydrogen bonding pattern of helix I caused by the binding of the secondary amine of **2c** to the heme iron. The methyl groups of the amine displace helix I. Carbon atoms are displayed in green for the **2b** complex or yellow for the **2c** complex. Nitrogen atoms are in blue, oxygen atoms are in red (**2b**) or green (**2c**), and the iron atom is in magenta.

Figure 3. 4,4′-Dipyridyl disulfide (DPD) interactions with CYP2A6. Carbon atoms are displayed in green for the DPD complex or white for the coumarin complex (PDB 1Z10). Nitrogen atoms are in blue, oxygen atoms are in red, and the iron and sulfur atoms are in orange. For clarity, coumarin is not included.

respectively. The structure of the CYP2A6 protein complexed with the primary amine was highly similar to that of the coumarin complex[15] indicating that little reorganization of the enzyme was required for binding of **2a**, the most potent of the three compounds. On the other hand, significant changes were evident in the structure of the enzyme for binding compounds **2b** and **2c** where the methyl groups from the secondary and tertiary amines displace Thr305 causing a turn in helix I to unwind and water molecules to bind in the cleft created (Figure 2). The distortion of helix I only slightly altered the position of Asn297, which maintained hydrogen bonds to a loop just after helix B′. The side-chain nitrogen of Asn297 was also positioned to donate a hydrogen bond to the aromatic nitrogen of the pyridyl ring. The nitrogen–nitrogen distances are 2.78 ± 0.05, 2.97 ± 0.04, and 2.97 ± 0.03 Å from the pyridyl nitrogen of **2a**, **2b**, and **2c**, respectively, to the side-chain nitrogen of Asn297. Phe118 repositions about 0.5 Å toward the pyridine moieties of **2b** and **2c** to maintain a face to edge aromatic interaction with each inhibitor, which may favor the observed orientation of the inhibitor.

The distortion in helix I caused by the methyl group(s) on the amine moieties of **2b** and **2c** mimics changes that are likely to occur when dioxygen binds to the iron of the reduced enzyme during the reaction cycle. A similar unwinding of the helix I occurs to accommodate the free end of the dioxygen molecule and permits water molecules to reside in the cleft of helix I, which may facilitate proton transfer to the distal oxygen of the reduced dioxygen molecule as described for P450 cam.[17,18]
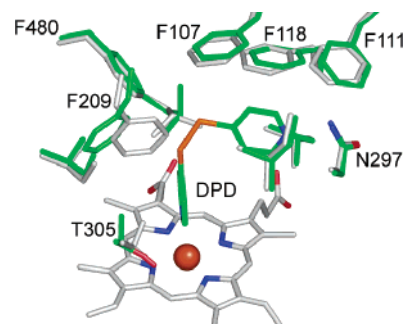
In comparison of the complexes of the three 3-heteroaromatic pyridine nicotine analogues with the complexes of coumarin and methoxsalen, the identities of CYP2A6 residues that contact the substrates are the same. Additionally, most of the changes in contact residue positions are restricted to slight rearrangements of the phenylalanine residues to maximize orthogonal aromatic interactions with the inhibitors. The active site volume of the complexes also remains similar to that of the coumarin complex at ~240−275 Å^3. This is in contrast to the complex of 4,4′-dipyridyl disulfide (Figure 3). To accommodate 4,4′-dipyridyl disulfide, the side chain of Phe209 moves away from the active site by ~3 Å relative to the coumarin complex to make room for the sulfur atoms of 4,4′-dipyridyl disulfide. This increases the active site volume to ~325 Å^3. The change in the active site provides clues as to how the protein can adapt to fit other larger molecules in the active site. The pyridyl nitrogen of one ring is positioned 2.30 ± 0.01 Å from the heme iron, and the bulky pryidyl ring also causes a repositioning of Thr301 and an opening of helix I with a concomitant occupancy of the cleft by two water molecules as was observed for the secondary and tertiary amines **2b** and **2c**. The other pyridyl nitrogen of 4,4′-dipyridyl disulfide is positioned 2.93 ± 0.13 Å from the side-chain nitrogen of Asn297 and is in a position to accept a hydrogen bond as seen for the 3-pyridyl ring of **2a**, **2b**, and **2c**. Thus, the changes in the active site maintain strong nitrogen coordination to the heme iron, a hydrogen bonding interaction with Asn297, and orthogonal aromatic–aromatic interactions between the inhibitor and protein side chains for all of these potent inhibitors. The high binding affinity for these relatively small molecules also likely stems from extensive van der Waals interactions between the protein and inhibitor and a significant

contribution from the hydrophobic effect arising from the displacement of water from the closed hydrophobic active site cavity.

The results clearly indicate that it is the side chain amino group of the three 3-heteroaromatic pyridine analogues of nicotine, **2a**, **2b**, and **2c**, that coordinates to the heme iron. This could reflect the importance of the hydrogen bonding and aromatic–aromatic interactions with the pyridine ring relative to any inherent difference in the affinity of the amino versus the pyridine nitrogen for coordination to the heme iron. The K_i values for **2a**, **2b**, and **2c** are 130 ± 10, 800 ± 170, and $14\,200 \pm 9200$ nM. The observed decrease in the binding affinity upon methylation of the amine from primary to tertiary amine could reflect in part the reorganization of the protein required to accommodate the methyl groups. It is also possible that these differences reflect in some degree the basicity of the aliphatic amino group. The latter could affect both the strength of the interaction with the heme iron and the ionization state of the inhibitor at physiological pH.

CYP Inhibition Selectivity. To explore further the selectivity of CYP2A6 inhibition, additional inhibitors (i.e., compounds **22**–**35**) were prepared and examined for their ability to inhibit selective functional activities of human CYP enzymes. The K_i values for inhibition of CYP2A6, -3A4, -2E1, -2B6, -2C9, -2C19, and -2D6 were reported in Table 2. The enzyme assays were done using standard conditions as previously described.[11] Compared with some of the most potent inhibitors previously described (i.e., pyridine-containing compounds **1a**, **2a**, **8**, and **11**), the corresponding phenyl compounds **22**–**25** decreased the inhibition of CYP2A6 between 4- and 7-fold. Thus, replacement of the pyridine with a phenyl substituent in this series attenuated the inhibitory potency toward CYP2A6. This suggests a significant contribution to the binding interaction between the inhibitor and CYP2A6 for the hydrogen bond between Asn297 and the pyridine nitrogen of **2a** and by inference the structural analogue **1a**. Likewise, for compounds **8** and **11**, which are less nucleophilic and without an amino functionality to ligate to the heme, substitution of a phenyl group for the pyridine moiety (i.e., in compounds **25** and **24**, respectively) leads to a type I spectral change suggesting that the inhibitor can no longer bind to the heme Fe. The pyridyl nitrogen of **8** and **11** may be oriented differently from that of **2a** (and oriented differently than **24** and **25**). For the other CYPs examined, generally, replacement of the pyridine for a phenyl group decreased inhibition markedly except for CYP2E1, CYP2B6, and CYP2C9 (Table 2). For compounds **22** and **23**, replacement of the pyridine nucleus by a phenyl group significantly increased inhibitory potency against CYP2E1, CYP2B6, and CYP2C9 (Table 2). Compound **23** was a potent inhibitor for CYP2E1 (i.e., $K_i = 43$ nM) but overall, compound **23** was not highly selective, because it also potently inhibited CYP2B6, CYP2C9, and CYP2C19. Compounds **22** and **23** were equally potent inhibitors of CYP2A6 but considerably less potent than the corresponding pyridine-containing compounds, **2a** and **1a**, respectively, illustrating the importance of the pyridine–Asn297 interaction for inhibitors with the correct overall dimensions.

Structure–Activity Studies. To further evaluate the SAR of the heteroaromatic portion of the inhibitor, the methylamino furan or methylamino thiophene moiety was replaced with different heterocycle-containing groups. Analogue **26**, with a 4-methylthiazol-2-yl moiety at the pyridine 3-position, possessed a K_i value of 4.1 μM. This is considerably less potent than the corresponding thiophene inhibitors (i.e., **4** and **7**) and suggests a methylthiazol group is less favored in this position. Analogue

27, with a 1*H*-pyrazol-3-yl group at the pyridine 3-position had a K_i value of 12.8 μM, which was considerably less potent than the corresponding imidazole-containing inhibitors (i.e., compounds **9** and **10**). Analogue **30**, which had a propan-1-amine moiety at the 3-position of pyridine in place of a heteroaromatic group, possessed a K_i value of 6.6 μM. This too was a considerably less potent inhibitor of CYP2A6 than inhibitors with 3-heteroaromatic groups or the inhibitor with an acetylenic group between the pyridine and the methylamino functionality (i.e., compound **3a**). Compound **30** may not span the correct distance between the heme iron and Asn297. To further probe the SAR of the heteroaromatic portion of the inhibitors, analogues **32** and **35** were prepared and tested. The 1*H*-pyrazol-5-yl- and isoxazol-5-yl-3-substituted pyridines (i.e., compounds **32** and **35**, respectively) possessed K_i values of 0.29 and 0.37 μM, respectively, against CYP2A6 and were considerably more potent inhibitors than the related imidazoles (i.e., compounds **10** and **27**). This suggests that CYP2A6 allows an additional heteroatom functionality in the five-membered heterocyle attached at the pyridine 3-position but these are less potent inhibitors compared to thiophenes and furans not substituted in the ring (i.e., compounds **1a** and **2a**). This result may underscore the hydrophobic nature of the active site and that even for inhibitors with H-bonding to Asn297 and ligation to the heme, additional interactions may play a role in modulating CYP2A6 inhibitory potency.

The analogues prepared were also examined for selectivity of CYP inhibition (Table 3). The CYP2A6 inhibitors were evaluated as inhibitors of CYP3A4, CYP2E1, CYP2B6, CYP2C9, CYP2C19, and CYP2D6 functional activity as described previously.[11] Full dose-range IC_{50} values were obtained and converted to the K_i values using the Cheng–Prusoff equation, and the CYP inhibition data was presented in Table 2. The selectivity ratios (i.e., $[K_i(CYPX)/K_i(CYP2A6)]$) are provided in Table 3. For the heterocycles substituted with a phenyl group instead of a pyridine moiety (i.e., compounds **22**–**25**), the CYPX/CYP2A6 selectivity ratios indicated much less selectivity for CYP2A6 than for the corresponding pyridine-substituted inhibitors (i.e., compounds **2a**, **1a**, **8**, and **11**, respectively) underscoring the importance of the pyridine nitrogen atom in CYP2A6 inhibition. Less potent CYP2A6 inhibitors (i.e., compounds **26**, **27**, and **30**) generally did not possess great selectivity ratios for CYP2A6 inhibition. The suggestion is that introduction of a 3-pyridine substituent alone in compounds **26**, **27**, and **30** did not contribute to increased potency nor selectivity for CYP2A6 inhibition. The more potent CYP2A6 inhibitors (i.e., compounds **32** and **35**) were quite selective for CYP2A6. Analogue **32** had selectivity ratios of >690, >690, 114, 83, 143, and 103 for CYP3A4, CYP2E1, CYP2B6, CYP2C9, CYP2C19, and CYP2D6, respectively. Analogue **35** had selectivity ratios of >541, 105, 91, 39, 74, and >541 for CYP3A4, CYP2E1, CYP2B6, CYP2C9, CYP2C19, and CYP2D6, respectively. Preliminary results (data not shown) showed that the compounds of Table 3 showed a distinct selectivity for inhibition of CYP2A13. On the basis of the selectivity ratios being >25 for each CYP, compounds **1b**, **8**, **32**, and **35** possessed significant utility as selective CYP2A6 inhibitors. Selective inhibition of CYP2A6 may result in the elaboration of agents capable of modulating nicotine self-administration in animals.

Conclusions

The chemical synthesis of the target compounds was achieved efficiently and afforded a number of highly potent and selective inhibitors of human CYP2A6. Most of the 3-heteroaromatic

pyridines that were potent inhibitors of CYP2A6 acted via a mechanism involving tight-binding competitive inhibition. However, several compounds showed time-dependent inhibition. The pyridine moiety was also found to be important for potent CYP2A6 inhibition. Substitution of a phenyl group for a pyridine (i.e., **11** to **24** or **8** to **25**) significantly decreased CYP2A6 inhibitory potency underscoring the importance of the pyridine−enzyme interaction. The most potent inhibitors had the pyridyl moiety positioned to accept a hydrogen bond from Asn297. Generally, appendage of an electron-rich moiety (i.e., amine, thiol, sulfide, etc.,) to the 3-heteroaromatic pyridine gave the most potent and selective inhibitors. Compounds **1a**, **2a**, **32**, and **35** were highly potent and selective inhibitors of CYP2A6. Preliminary studies have also shown that the most potent CYP2A6 inhibitors are not the most potent CYP2A13 inhibitors. Because CYP2A13 is the major form of CYP2A in the human lung, this may suggest that it may be possible to develop isoform- and tissue-selective inhibitors of CYP2A. For CYP2A6 inhibitors, an electron-rich center coordinates to the heme iron and the pyridine nitrogen H-bonds to Asn297. Cocrystallization studies bear out these mechanistic points and further illustrate the importance of aromatic and hydrophobic interactions and movement of water in the active site of CYP2A6 as a consequence of inhibitor binding.

The dose−response relationship between the number of cigarettes smoked and the development of lung cancer was established many years ago by epidemiological studies.[19] Decreasing smoking and developing approaches to decrease the toxicity, addiction liability, and carcinogenicity of cigarettes will result in fewer lung cancer deaths. One approach to decrease smoking is to develop an agent that replaces nicotine and that inhibits the formation of nicotine-related carcinogens. Development of potent and selective inhibitors of human CYP2A6 may provide insight into small molecules that could be used as smoking cessation agents.

Materials and Methods

Materials. The synthesis of test compounds **1a**−**1c**, **2a**−**2c**, **3a**−**3c**, and **4**−**11** has been previously reported.[11] All commercially available reagents and chemicals were purchased from Aldrich Chemical Co. or VWR and were used as received. Moisture-sensitive reactions were carried out in flame-dried glassware under an argon atmosphere. Tetrahydrofuran (THF) and toluene were freshly distilled from calcium hydride under an argon atmosphere. Methanol (CH_3OH) was passed through a column of neutral alumina and stored over 3 Å molecular sieves prior to use. Melting points were determined on a Mettler-Toledo FP62 melting point instrument and were uncorrected. Analytical thin-layer chromatography (TLC) was done on K6F silica gel 60 Å (Whatman) glass-backed plates. Compounds were detected using UV absorption at 254 nm or stained with I_2 (iodine). Flash chromatography was performed on Merck (60 Å) pore silica. NMR spectra were recorded at 300 MHz on a Varian Mercury spectrometer. Chemical shifts are reported in parts per million (ppm, δ) using residual solvent signals as internal standards. Mass spectroscopy was done using electrospray ionization (ESI) on a Hitachi M-8000 3DQMS (ion trap) mass spectrometer. High-resolution mass spectrometry was done on a Waters LCT Premier instrument operating in the ESI mode, and GCMS was done on a Therm Trace instrument operating in the electron impact (EI) mode at the University of California, Irvine. UV spectral data was acquired on a Varian Cary 1E UV−visible spectrophotometer.

Microsomes from human lymphoblast cells expressing human cytochrome P-450 2A6 and human liver microsomes (CYP3A4) were purchased from BD Gentest (Woburn, MA), and microsomes from baculovirus-infected cells coexpressing cytochrome P-450s (2E1, 2B6, 2C9, 2C19 and 2D6), NADPH-cytochrome P-450 reductase, and cytochrome b_5 (BACULOSOMES) were purchased from PanVera LLC (Madison, WI).

Crystallization of CYP2A6/Inhibitor Complexes. For crystallization of CYP2A6−inhibitor complexes, a modified form of the protein was used where the N-terminal transmembrane region was replaced with a short hydrophilic sequence optimized for expression of the protein in *Escherichia coli*.[20] The construct (i.e., CYP2A6dH) also included a four-residue histidine tag at the C-terminus to facilitate purification.[21] CYP2A6dH was crystallized in the presence of a 2-fold molar excess of each inhibitor by sitting drop vapor diffusion as described previously for the coumarin and methoxsalen complexes, with slight modifications to optimize crystal growth.[15] Data were collected from single crystals at Stanford Synchrotron Radiation Laboratory on beamline 9-1. All data were reduced and scaled in either HKL2000/Scalepack[22] or Mosflm/Scala.[23] The data were phased initially by isomorphous replacement using the previously determined structure of CYP2A6dH, PDB 1Z10. The protein and inhibitor structures were fit to electron density maps using the computer program O[24] and refined using CNS.[21] Data reduction and structure refinement statistics are presented in Table 4.

Chemical Synthesis. 3-(Pyridin-3-yl)prop-2-yn-1-amine (**3a**), *N*-methyl-3-(pyridin-3-yl)prop-2-yn-1-amine (**3b**), and *N*,*N*-dimethyl-3-(pyridin-3-yl)prop-2-yn-1-amine (**3c**) were synthesized as previously described and gave the following HRMS: (**3a**) HRMS (ESI) m/z calcd for $C_8H_9N_2$ [M + H]$^+$ 133.0766, found 133.0767; (**3b**) HRMS (ESI) m/z calcd for $C_9H_{10}N_2$ [M + H]$^+$ 147.0922, found 147.0920; (**3c**) HRMS (ESI) m/z calcd for $C_{10}H_{13}N_2$ [M + H]$^+$ 161.1079, found 161.1074.

(5-(Pyridin-3-yl)furan-2-yl)methanol (12). To a slurry of **16** (54 mg, 0.31 mmol) in CH_3OH (5 mL) was added sodium borohydride (12 mg, 0.31 mmol) in one portion, and the resultant solution was stirred at room temperature for 10 min. The reaction was stopped by the addition of aqueous sodium bicarbonate (50: 50 satd. soln./water, v/v), and the CH_3OH was removed in vacuo. The residue was partitioned between water (20 mL) and ether (20 mL), the organic layer was collected, and the aqueous fraction was re-extracted with ether (2 × 20 mL). The combined organic portions were washed with water (20 mL), dried ($MgSO_4$), filtered, and concentrated in vacuo to afford the title compound **12** (50 mg, 92% yield) as an off white solid: mp = 119−120 °C; ^{1}H NMR (CDCl$_3$, 500 MHz) δ 8.88 (s, 1H), 8.42 (m, 1H), 7.88 (m, 1H), 7.27, (m, 1H), 6.65 (d, *J* = 3.1 Hz, 1H), 6.38 (d, *J* = 3.1 Hz, 1H), 4.66 (s, 2H); LRMS (ESI) m/z calcd for $C_{10}H_{10}NO_2$ [M + H]$^+$ 176, found 176; HRMS (ESI) m/z calcd for $C_{10}H_{10}NO_2$ [M + H]$^+$ 176.0712, found 176.0694.

***S*-(5-(Pyridin-3-yl)furan-2-yl)methyl ethanethioate (13).** To a solution of alcohol **12**[11] (121 mg, 0.69 mmol) in CH_2Cl_2 (5 mL) at 0 °C under an argon atmosphere was added phosphorus tribromide (0.03 mL, 0.34 mmol) dropwise over 10 min; the ice bath was removed, and the resultant solution was stirred at ambient temperature for 24 h, heated to reflux, and stirred for 1.5 h (Scheme 1). The solution was cooled to room temperature, diluted with CH_2Cl_2 (50 mL), washed with aqueous sodium bicarbonate (50:50, satd. soln./water, v/v, 3 × 10 mL), dried (Na_2SO_4), and filtered, and the solvent was removed in vacuo. The residue was taken up in DMF (5 mL), treated with potassium thioacetate (95 mg, 0.83 mmol), heated to 100 °C, and stirred overnight. The solution was cooled to room temperature, poured into aqueous sodium bicarbonate (50: 50, satd. soln./water, v/v, 30 mL), extracted with EtOAc (3 × 30 mL), back-washed with aqueous sodium bicarbonate (50:50, satd. soln./water, v/v, 2 × 20 mL) and brine (1 × 20 mL), dried (Na_2-SO_4), and filtered, and the solvent was removed in vacuo. The crude material was chromatographed on silica gel (EtOAc/Hex, 25:75, v/v, R_f = 0.18) to afford the title compound **13** (43 mg, 27% yield) as a yellow semisolid: ^{1}H NMR (CD$_3$OD) δ 8.87 (br s, 1H), 8.48 (br s, 1H), 7.89 (m, 1H), 7.30 (m, 1H), 6.64 (d, *J* = 3.3 Hz, 1H), 6.34 (d, *J* = 3.0 Hz, 1H), 4.20 (s, 2H), 2.37 (s, 3H); LRMS (ESI) m/z calcd for $C_{12}H_{12}NO_2S$ [M + H]$^+$ 234, found 234.

(5-Pyridin-3-yl-furan-2-yl)methanethiol (14). To a solution of **13** (10 mg, 0.05 mmol) in CHCl$_3$/CH$_3$OH (1.5 mL, 2:1, v/v) was added sodium thiomethoxide (3 mg, 0.05 mmol), and the resultant solution was stirred under argon for 10 min. The solvent was

removed with a stream of argon, and the residue was applied directly to a TLC plate (20 × 20 cm, 250 μm silica gel) and developed with an eluant of EtOAc/Hex (5:95, v/v, R_f = 0.12). The product band was scraped and eluted with dichloromethane, and the solvent was removed in vacuo to afford the title compound **14** (6 mg, 68% yield) as a white film: ^{1}H NMR (CD$_3$OD) δ 8.72 (m, 1H), 8.19 (m, 1H), 7.96 (m, 1H), 7.28 (m, 1H), 6.66 (d, J = 3.3 Hz, 1H), 6.07 (d, J = 3.3 Hz, 1H), 3.59 (s, 2H), LRMS (ESI) m/z calcd for C$_{10}$H$_{10}$NOS [M + H]$^+$ 192, found 192.

3-(5-((Methylthio)methyl)furan-2-yl)pyridine (15). To a solution of **13** (27 mg, 0.12 mmol) in anhydrous CH$_3$OH (3 mL) at 0 °C under argon was added dropwise a solution of sodium methoxide (15 mg, 0.28 mmol) in anhydrous CH$_3$OH (1 mL) over 10 min, and the resultant solution was stirred for 30 min. To the resultant solution was added dropwise methyl iodide (17 μL, 0.28 mmol) in anhydrous CH$_3$OH (1 mL) over 1 min, and the resultant solution was stirred for 30 min. The reaction was stopped by the addition of aqueous sodium bicarbonate (satd. soln., 10 mL). CH$_3$OH was removed in vacuo, and the aqueous fraction was extracted with EtOAc (3 × 10 mL). The combined organic fractions were dried (Na$_2$SO$_4$) and filtered, and the solvent was removed in vacuo. The crude material was chromatographed on silica gel (EtOAc/Hex, 25:75, v/v, R_f = 0.2) to afford the title compound **15** (13 mg, 54% yield) as an off white solid: mp = 67−68 °C; ^{1}H NMR (CDCl$_3$) δ 8.90 (br s, 1H), 8.46 (m, 1H), 7.90 (m, 1H), 7.29 (m, 1H), 6.66 (d, J = 3.3 Hz, 1H), 6.29 (d, J = 3.3 Hz, 1H), 3.74 (s, 2H), 2.14 (s, 3H); LRMS (ESI) m/z calcd for C$_{11}$H$_{12}$NOS [M + H]$^+$ 206, found 206.

5-(Pyridin-3-yl)furan-2-carbaldehyde (16). The general Suzuki coupling procedure was followed. The crude material was chromatographed on silica gel (EtOAc/Hex, 50:50, R_f = 0.19) to afford the title compound **16** (1.28 g, 95% yield) as an off white solid. Analytical properties are consistent with published values: mp = 112−115 °C (lit. 113−115 °C);[11] ^{1}H NMR (CDCl$_3$) δ 9.70 (s, 1H), 9.05 (m, 1H), 8.63 (m, 1H), 8.12 (m, 1H), 7.39 (m, 1H), 7.35 (d, J = 4.1 Hz, 1H), 6.94 (d, J = 4.1 Hz, 1H).

3-(5-[1,3]Dithiolan-2-yl-furan-2-yl)pyridine (17). To a solution of aldehyde **16**[11] (44 mg, 0.25 mmol) in anhydrous toluene (5 mL) was added ethane dithiol (21 μL, 0.25 mmol) followed by toluenesulfonic acid (approximately 2 mg), and 4 Å molecular sieves, and the resultant solution was stirred under nitrogen overnight. An additional 5 mg of toluenesulfonic acid was added, and the solution was stirred under argon for 2 h. The toluene was decanted, and the resulting residue was rinsed with hexanes. The residue was partitioned between EtOAc (20 mL) and aqueous sodium bicarbonate (satd. soln., 20 mL). The organic fraction was collected, and the aqueous fraction was extracted with EtOAc (2 × 20 mL). The combined organic fractions were dried (Na$_2$SO$_4$) and filtered, and the solvent was removed in vacuo. The crude material was chromatographed on silica gel (EtOAc/Hex, 50:50, v/v, R_f = 0.3) to afford the title compound **17** (10 mg, 83% yield) as a yellow film: ^{1}H NMR (CDCl$_3$) δ 8.88 (m, 1H), 8.47 (m, 1H), 8.89 (m, 1H), 7.28 (m, 1H), 6.63 (m, 1H), 6.41 (m, 1H), 5.65 (s, 1H), 3.50−3.30 (m, 4H); LRMS (ESI) m/z calcd for C$_{12}$H$_{12}$NOS$_2$ [M + H]$^+$ 250, found 250.

General Procedure for Suzuki Coupling Reactions. To a dry glass vial purged with argon containing a magnetic stir bar was added the heteroarylbromide (1.3 mmol). To the vial was added a solution of tetrakis(triphenylphosphine)palladium(0) (0.03 mmol) in dimethoxyethane (2 mL) and sodium carbonate (aq) (2 M, 1.3 mL, 2.6 mmol), and the vial was once again purged with argon. The resultant solution was stirred at room temperature for 5 min, and a solution of phenylboronic acid (198 mg, 1.63 mmol) in ethanol (2 mL) was added; the vial was purged with argon, capped, heated to 90 °C, and stirred for 1 h (Scheme 2). The solution was cooled to room temperature and filtered through a pad of Celite by washing with dichloromethane and dried with anhydrous magnesium sulfate (5 g). The solution was then filtered through filter paper, and the solvent was removed in vacuo to afford the crude product, which was chromatographed on silica gel.

5-Phenylfuran-2-carboxaldehyde (18). The general Suzuki coupling procedure was followed. The crude material was chromatographed on silica gel (EtOAc/Hex, 10:90, v/v, R_f = 0.21) to afford the title compound **18** (201 mg, 90% yield) as an orange oil: ^{1}H NMR (CDCl$_3$) δ 9.59 (s, 1H), 7.75 (m, 2H), 7.36 (m, 3H), 7.26 (d, J = 3.9 Hz, 1H), 6.78 (d, J = 3.6 Hz, 1H); LRMS (ESI) m/z calcd for C$_{11}$H$_9$O$_2$ [M + H]$^+$ 173, found 173.

5-Phenylthiophene-2-carboxaldehyde (19). The general Suzuki coupling procedure was followed. The crude material was combined and chromatographed on silica gel (EtOAc/Hex, 10:90, v/v, R_f = 0.16) to afford the title compound **19** (410 mg, 84% yield) as a yellow solid: mp = 92−93 °C; ^{1}H NMR (CDCl$_3$) δ 9.88 (s, 1H), 7.74 (d, J = 3.8 Hz, 1H), 7.68−7.65 (m, 2H), 7.46−7.39 (m containing a doublet, J = 3.9 Hz, 4H); LRMS (ESI) m/z calcd for C$_{11}$H$_9$OS [M + H]$^+$ 189, found 189.

***cis/trans*-5-Phenylfuran-2-carbaldehyde Oximes (20).** To a solution of **18** (220 mg, 1.28 mmol) in 95% ethanol (6 mL) was added hydroxylamine hydrochloride (107 mg, 1.53 mmol) and sodium acetate (126 mg, 1.53 mmol), and the resultant slurry was heated to reflux and stirred for 25 min. The slurry was diluted with EtOAc (20 mL), washed with water (3 × 20 mL), dried (Na$_2$SO$_4$), and filtered, and the solvent was removed in vacuo to afford a cis/trans mixture of the compound **20** (228 mg, 95% yield) as a yellow semisolid that was used in further reactions without further purification: ^{1}H NMR (CD$_3$OD) δ 7.99 (s, 1.3H), 7.76−7.71 (m, 5H), 7.48 (s, 0.7H), 7.42−7.24 (m, 7H), 6.89−6.71 (m, 4H); LRMS (ESI) m/z calcd for C$_{11}$H$_{10}$NO$_2$ [M + H]$^+$ 188, found 188.

***cis/trans*-5-Phenylthiophene-2-carboxaldehyde oxime (21).** To a solution of **19** (193 mg, 1.03 mmol) in 95% ethanol (5 mL) was added hydroxylamine hydrochloride (86 mg, 1.23 mmol) and sodium acetate (100 mg, 1.23 mmol), and the resultant slurry was heated to reflux and stirred for 25 min. The slurry was poured into water (25 mL), extracted with EtOAc (3 × 25 mL), dried (Na$_2$SO$_4$), and filtered, and the solvent was removed in vacuo to afford the cis/trans mixture of the title compound **21** (228 mg, 95% yield) as a yellow solid, which was used in further reactions without further purification: mp = 136−138 °C; ^{1}H NMR (CDCl$_3$) δ 8.27 (s, 1H), 7.72 (s, 1H), 7.68−7.60 (m, 5H), 7.40−7.29 (m, 9H) 7.24 (d, J = 3.8 Hz, 1H), 7.16 (d, J = 3.8 Hz, 1H); LRMS (ESI) m/z calcd for C$_{11}$H$_{10}$NO$_2$ [M + H]$^+$ 204, found 204.

(5-Phenylfuran-2-yl)methanamine (22). To a solution of **20** (95 mg, 0.51 mmol) in THF (5 mL) was added dropwise a solution of lithium aluminum hydride (1.0 M, 0.63 mL, 0.63 mmol), and the resultant solution was stirred at room temperature for 24 h. The reaction was poured into MeOH (20 mL), diluted with water (50 mL), extracted with CHCl$_3$/IPA (3:1, 50 mL, 2 × 20 mL), dried (Na$_2$SO$_4$), and filtered, and the solvent was removed in vacuo to afford the title compound **22** (46 mg, 52% yield) as a colorless oil. Compound **22** was not indefinitely stable and therefore was converted to the more stable hydrochloride salt. Thirty-five milligrams of **22** was dissolved in dry Et$_2$O (2 mL) and treated with ethereal HCl (1 mL). The solid was collected by filtration to afford the hydrochloride salt of **22** (12 mg) as an off-white foam: ^{1}H NMR (D$_2$O) δ 7.59 (m, 2H), 7.29 (m, 2H), 7.19 (m, 1H), 6.64 (d, J = 3.3, 1H), 6.45 (d, J = 3.6, 1H), 4.09 (s, 2H); LRMS (ESI) m/z calcd for C$_{11}$H$_9$O [M − NH$_2$]$^+$ 157, found 157.

(5-Phenylthiophen-2-yl)methanamine (23). To a solution of **21** (150 mg, 0.74 mmol) in THF (5 mL) was added dropwise a solution of lithium aluminum hydride (1.0 M, 0.92 mL, 0.92 mmol), and the resultant solution was stirred at room temperature for 24 h. The reaction was poured into MeOH (20 mL), diluted with water (50 mL), extracted with CHCl$_3$/IPA (3:1, 50 mL, 2 × 20 mL), dried (Na$_2$SO$_4$), and filtered and the solvent was removed in vacuo. The crude material was chromatographed on silica gel (preparative TLC, CH$_3$OH/CHCl$_3$, 10:90, v/v, R_f = 0.18) to afford the title compound **23** (11 mg, 8% yield) as a white film: ^{1}H NMR (CDCl$_3$) δ 7.58−7.55 (m, 2H), 7.38−7.33 (m, 2H), 7.28−7.23 (m, 1H), 7.14 (d, J = 3.6, 1H), 6.87 (d, J = 3.6, 1H), 4.05 (s, 2H); LRMS (ESI) m/z calcd for C$_{11}$H$_9$S [M − NH$_2$]$^+$ 173, found 173. HRMS (ESI) m/z calcd for C$_{11}$H$_{12}$NS [M + H]$^+$ 190.2825, found 190.2826.

3-Methyl-4-phenylthiophene (24). The general Suzuki coupling procedure was followed (Scheme 3). The crude material was chromatographed on silica gel (hexane, $R_f = 0.4$) to afford the title compound **24** (203 mg, 90% yield) as a colorless oil: ^{1}H NMR (CDCl$_3$) δ 7.46−7.35 (m, 5H), 7.23 (d, $J = 3.3$ Hz, 1H), 7.06 (m, 1H), 2.32 (s, 3H). HRMS (ESI) m/z calcd for C$_{10}$H$_9$ S [M + H]$^+$ 161.0425, found 161.0419.

3-Phenylthiophene (25). The general Suzuki coupling procedure was followed. The crude material was chromatographed on silica gel (hexane, $R_f = 0.44$) to afford the title compound **25** (183 mg, 90% yield) as a white solid. The analytical data was consistent with previously published values.[25] Electron impact GCMS showed that the compound was >99% pure. LRMS m/z calcd for C$_{11}$H$_{10}$S 117, found 117.

3-(4-Methylthiazol-2-yl)pyridine (26). To a slurry of thionicotinamide (3.3 g, 23.9 mmol) in ethanol (100 mL) was added chloroacetone (2.28 mL, 28.7 mmol), and the resultant material was heated to reflux and stirred for 48 h (Scheme 4). The solvent was removed in vacuo, and the crude material was chromatographed on silica gel (EtOAc/Hex, 50:50, v/v, $R_f = 0.34$) to afford the title compound **26** (543 mg, 13% yield) as a brown solid: mp = 42−43 °C; ^{1}H NMR (CDCl$_3$) δ 9.09 (m, 1H), 8.57 (m, 1H), 8.15 (m, 1H), 7.31 (m, 1H), 6.89 (m, 1H), 2.47 (s, 3H); LRMS (ESI) m/z calcd for C$_9$H$_8$N$_2$S [M + H]$^+$ 177, found 177; HRMS (ESI) m/z calcd for C$_9$H$_9$N$_2$S [M + H]$^+$ 177.2435, found 176.2431.

3-(1H-Pyrazol-3-yl)pyridine (27). To a solution of nicotinaldehyde (2.0 mL, 21.2 mmol) in 95% EtOH (20 mL) was added 2-tosylhydrazine (3.95 g, 21.2 mmol), and the resultant solution was stirred at room temperature for 2 h. To the solution was added aqueous sodium hydroxide (5 N, 4.2 mL, 21.2 mmol), and the solution was stirred for 20 min. To the solution was added 1-vinylimidazole (9.6 mL, 106 mmol), and the resultant solution was warmed to 50 °C and stirred under an argon atmosphere for 96 h. The solution was poured into a water/EtOAc mixture (1:1, v/v, 100 mL), the organic fraction was collected, and the aqueous fraction was extracted with EtOAc (2 × 50 mL). The combined organic fractions were dried (Na$_2$SO$_4$) and filtered, and the solvent was removed in vacuo. The crude material was chromatographed on silica gel (EtOAc/Hex, 50:50, v/v, $R_f = 0.08$) to afford the title compound **27** (1.73 g, 56% yield) as a pale white oil: ^{1}H NMR (CDCl$_3$) δ 9.03 (m, 1H), 8.52 (m, 1H), 8.06 (m, 1H), 7.59 (d, $J = 2.2$ Hz, 1H), 7.29 (m, 1H), 6.61 (d, $J = 2.5$ Hz, 1H); LRMS (ESI) m/z calcd for C$_8$H$_8$N$_3$ [M + H]$^+$ 146, found 146; HRMS (ESI) m/z calcd for C$_8$H$_8$ N$_3$ [M + H]$^+$ 146.0718, found 146.0720.

(3-Pyridin-3-yl-prop-2-ynyl)-carbamic Acid tert-Butyl Ester (28). To a vial containing 3-bromopyridine (513 mg, 3.3 mmol) was added a solution of tetrakis(triphenylphosphine)palladium(0) (90.1 mg, 0.08 mmol) in dimethoxyethane (2 mL) and sodium carbonate (aq) (2 M, 2.6 mL, 5.2 mmol) and the vial was once again purged with argon. To the solution was added tert-butyl prop-2-ynyl carbamate (403.5 mg, 2.6 mmol) in dimethoxyethane (3 mL), and the mixture was stirred vigorously. Next, the solution was cooled to 0 °C, and CuI (79.3 mg, 0.42 mmol) was added; the ice bath was removed, and the solution was warmed and stirred at 90 °C for 1 h. After the reaction was cooled, saturated aqueous sodium bicarbonate (10 mL) was added, the organic material was collected, and the aqueous fraction was extracted with CH$_2$Cl$_2$ (2 × 15 mL), back-washed with water (30 mL) and brine (30 mL), dried (Na$_2$SO$_4$), and filtered, and the solvent was removed in vacuo. The crude material was chromatographed on silica gel (EtOAc/Hex, 35:65, v/v, $R_f = 0.17$) to afford the title compound **28** (510 mg, 84% yield) as a yellow solid: mp 140−144 °C dec; ^{1}H NMR (CDCl$_3$) δ 8.39 (s, 1H), 7.63 (m, 1H), 7.21 (m, 2H), 4.9 (br s, 1H), 4.1 (d, 2H) 1.44 (s, 9H); LRMS (ESI) m/z calcd for C$_{13}$H$_{16}$N$_2$O$_2$ [M + H]$^+$ 233, found 233; HRMS (ESI) m/z calcd for C$_{13}$H$_{16}$N$_2$O$_2$ [M + H]$^+$ 233.2832, found 233.2829.

tert-Butyl 3-(Pyridin-3-yl)propylcarbamate (29). To a solution of acetylene **28** (255 mg, 1.2 mmol) in CH$_3$OH (20 mL) was added a slurry of 10% Pd/C (60 mg) in CH$_3$OH (5 mL). The resultant solution was degassed and purged with hydrogen three times and then hydrogenated under balloon pressure for 24 h. The catalyst

was removed by filtration through a pad of Celite, and the solvent was removed in vacuo to afford the title compound **29** (TLC, EtOAc/Hex, 50:50, v/v, $R_f = 0.16$) (249 mg, 97% yield) as a pale yellow oil: ^{1}H NMR (CDCl$_3$) δ 8.31 (m, 2H), 7.41 (m, 1H), 7.10 (m, 1H), 5.08 (br s, 1H), 3.04 (br q, $J = 12.9$, 6.6 Hz, 2H), 2.53 (t, $J = 7.8$ Hz, 2H), 6.18 (heptet, $J = 15.1$, 7.4 Hz, 2H), 1.33 (s, 9H); LRMS (ESI) m/z calcd for C$_{13}$H$_{21}$N$_2$O$_2$ [M + H]$^+$ 237, found 237.

3-(Pyridin-3-yl)propan-1-amine (30). To a solution of **29** (249 mg, 1.05 mmol) in CH$_2$Cl$_2$ (3 mL) at 0 °C was added excess TFA (2 mL); the ice bath was removed, and the resultant solution was stirred at ambient temperature for 1 h. The solvent and excess TFA were removed with a stream of nitrogen, and the residue was partitioned between HCl(aq) (1.0 M, 2 mL) and EtOAc (10 mL). The aqueous fraction was collected and subsequently washed with EtOAc (2 × 10 mL). To the remaining aqueous fraction was added CH$_2$Cl$_2$ (20 mL) and water (20 mL), and the pH was adjusted to 10 with NaOH(aq) (10 N) while stirring. The organic fraction was collected, and the remaining aqueous fraction was extracted with CH$_2$Cl$_2$ (2 × 15 mL). The combined organic fractions were dried (Na$_2$SO$_4$) and filtered, and the solvent was removed in vacuo to afford the title compound **30** (97 mg, 68% yield) as a yellow oil: ^{1}H NMR (CDCl$_3$) δ 8.35 (m, 2H), 7.42 (m, 1H), 7.12 (m, 1H), 2.67−2.54 (m, 4H), 1.73−1.63 (m, 4H); LRMS (ESI) m/z calcd for C$_8$H$_{13}$N$_2$ [M + H]$^+$ 137, found 137. HRMS (ESI) m/z calcd for C$_8$H$_{13}$ N$_2$ [M + H]$^+$ 137.1079, found 137.1073.

tert-Butyl(3-(pyridin-3-yl)-1H-pyrazol-5-yl)methyl Carbamate (31). To a solution of nicotinaldehyde (150 μL, 1.59 mmol) in 95% EtOH (5 mL) was added 2-tosylhydrazine (296 mg, 1.59 mmol), and the resultant solution was stirred at room temperature for 2 h (Scheme 5). To the solution was added aqueous sodium hydroxide (5 N, 0.32 mL, 1.59 mmol), and the solution was stirred for 20 min. To the solution was added a solution of tert-butyl prop-2-ynyl carbamate (1.23 g, 7.95 mmol), and the resultant solution was warmed to 50 °C and stirred under an argon atmosphere for 96 h. The solution was poured into a water/EtOAc mixture (1:1, v/v, 100 mL), the organic fraction was collected, and the aqueous fraction was extracted with EtOAc (2 × 20 mL). The combined organic fractions were dried (Na$_2$SO$_4$) and filtered, and the solvent was removed in vacuo. The crude material was chromatographed on silica gel (EtOAc/Hex, 50:50, v:v, $R_f = 0.08$) to afford the title compound **31** (158 mg, 36% yield) as a white solid: mp = 185−187 °C; ^{1}H NMR (CDCl$_3$) δ 8.92 (m, 1H), 8.50 (m, 1H), 8.01 (m, 1H), 7.28 (m, 1H), 6.47 (s, 1H), 5.62 (br s, 1H), 4.34 (d, $J = 6$ Hz, 1H), 1.45 (s, 9H); LRMS (ESI) m/z calcd for C$_{14}$H$_{19}$N$_4$O$_2$ [M + H]$^+$ 275, found 275.

(3-(Pyridin-3-yl)-1H-pyrazol-5-yl)methanamine (32). To a solution of **31** (40 mg, 0.11 mmol) in CH$_2$Cl$_2$ (1 mL) at 0 °C was added excess TFA (1 mL), and the resultant solution was stirred for 30 min. The solvent and excess TFA were removed under a stream of nitrogen, and the residue was partitioned between HCl-(aq) (1.0 M, 1 mL) and Et$_2$O (5 mL). The aqueous fraction was collected and subsequently washed with Et$_2$O (2 × 5 mL). To the remaining aqueous fraction was added CHCl$_3$ (10 mL) and water (10 mL), and the pH was adjusted to 10 with 10 N NaOH(aq) while stirring. The organic fraction was collected, and the remaining aqueous fraction was extracted with CHCl$_3$ (2 × 10 mL). The combined organic fractions were dried (Na$_2$SO$_4$) and filtered, and the solvent was removed in vacuo to afford the title compound **32** (3.4 mg, 14% yield) as a colorless oil: ^{1}H NMR (CDCl$_3$) δ 8.99 (m, 1H), 8.55 (m, 1H), 8.08 (m, 1H), 7.32 (m, 1H), 6.49 (s, 1H), 4.05 (s, 2H); LRMS (ESI) m/z calcd for C$_9$H$_{11}$N$_4$ [M + H]$^+$ 175, found 175; HRMS (ESI) m/z calcd for C$_9$H$_{11}$N$_4$ [M + H]$^+$ 175.2127, found 175.2124.

Nicotinaldehyde Oxime (33). Nicotinaldehyde oxime was prepared in quantitative yield by the reaction of nicotinaldehyde with hydroxylamine and sodium acetate in ethanol as described above for **20**.

tert-Butyl (3-(Pyridin-3-yl)isoxazol-5-yl)methylcarbamate (34). To a solution of **33** (161 mg, 1.3 mmol) in anhydrous DMF (5 mL) at 0 °C was added N-chlorosuccinimide (202 mg, 1.3 mmol) portionwise over 20 min. The resultant solution was heated to 50

°C and stirred for 50 min. The solution was cooled at room temperature and transferred to a flask containing CH_2Cl_2 (3 mL). To the solution was added a solution of *tert*-butyl prop-2-ynyl carbamate (204 mg, 1.3 mmol) in CH_2Cl_2 (3 mL), the solution was cooled to 0 °C, and triethylamine (0.18 mL, 1.3 mmol) was added dropwise. The ice bath was removed, and the solution was stirred at ambient temperature for 3 h. To the solution was added saturated aqueous sodium bicarbonate (30 mL), the organic fraction was collected, and the aqueous fraction was extracted with CH_2Cl_2 (2 × 15 mL), back-washed with water (30 mL) and brine (30 mL), dried (Na_2SO_4) and filtered. The solvent was removed in vacuo. The crude material was chromatographed on silica gel (EtOAc/ Hex, 50:50, v/v, $R_f = 0.16$) to afford the title compound **34** (212 mg, 59% yield) as a an off white solid: mp = 67−69 °C; ^1H NMR ($CDCl_3$) δ 8.93 (br s, 1H), 8.62 (m, 1H), 8.05 (m, 1H), 7.34 (m, 1H), 6.5 (s, 1H), 5.63 (br s, 1H), 4.43 (d, $J = 6$ Hz, 1H), 1.4 (s, 9H); LRMS (ESI) m/z calcd for $C_{14}H_{18}N_3O_3$ [M + H]$^+$ 276, found 276.

(3-(Pyridin-3-yl)isoxazol-5-yl)methanamine Dihydrochloride (35). To a solution of **34** (67 mg, 0.24 mmol) in 1,4-dioxane (5 mL) at 0 °C was bubbled HCl(g) until the solution was saturated. The ice bath was removed, and the solution was stirred at ambient temperature for 2 h. The solvent and excess HCl were removed with a stream of argon to afford the title compound **35** (45 mg, 88% yield) as a white solid: mp = 153−155 °C dec; ^1H NMR (D_2O) δ 9.12 (m, 1H), 8.83 (m, 1H), 8.73 (m, 1H), 8.04 (m, 1H), 7.04 (s, 1H), 4.35 (s, 2H); LRMS (ESI) m/z calcd for $C_9H_{10}N_3O$ [M + H]$^+$ 176, found 176; HRMS (ESI) m/z calcd for $C_9H_{11}N_3O$ [M + H]$^+$ 176.0824, found 176.0825.

CYP Inhibition Assays. To measure CYP2A6 and CYP3A4 activity, coumarin 7-hydroxylation and testosterone 6-hydroxylation, respectively, was determined as previously described.[11] To measure CYP2E1, CYP2B6, CYP2C9, CYP2C19, and CYP2D6 activity, isozyme specific Vivid Blue substrate O-dealkylation was determined via a modified Panvera Vivid Assay Protocol as previously described.[11]

Mouse and Human Liver Microsome Stability Assays. A typical assay mixture contained mouse or human liver microsomes (0.4−0.5 mg of protein), 100 μM potassium phosphate buffer (pH 7.4), 40 μM test compound, an NADPH-generating system consisting of 0.5 mM NADP$^+$, 0.5 mM glucose-6-phosphate, 5 U/mL glucose-6-phosphate dehydrogenase, 1 mg/mL diethylenetriamine-pentaacetic acid (DETAPAC), and 7 mM $MgCl_2$ for a final incubation volume of 0.1 mL. Incubations were run for 0, 10, 25, 40, and 60 min with shaking at 37 °C in a water bath and were terminated by the addition of 1 mL of CH_2Cl_2/2-propanol (3:1, v/v). After centrifugation at 13 000 rpm for 5 min, the organic fraction was collected, and the solvent was removed with a stream of argon. The residue was reconstituted in methanol (200 μL) centrifuged at 13 000 rpm for 5 min, and the supernatant was analyzed by high-performance liquid chromatography with an Axxi-chrom (straight-phase) silica column (4.6 mm × 250 mm, 5 μm) or with a Supelco (reverse-phase) HS F5 pentafluorophenyl column (4.6 mm × 250 mm, 5 μm). Standard conditions utilized an isocratic, ternary-solvent system consisting of solvents A (methanol), B (2-propanol), and C (aqueous 70% $HClO_4$) set at a flow rate of 1.5 mL/min (straight-phase), or A, D (water), and E (HCO_2H) set at a flow rate of 1.0 mL/min (reverse-phase), λ = 254 nm with retention times (t_R) evaluated in min. The specific conditions and retention times of each individual compound are specified in the Supporting Information.

Time-Dependent Inhibition of CYP2A6. The incubation mixture contained CYP2A6 supersomes (1 pmol protein), an NADPH-generating system consisting of 0.5 mM NADP$^+$, 0.5 mM glucose-6-phosphate, 5 U/mL glucose-6-phosphate dehydrogenase, and 1 mg/mL DETAPAC. The preincubation was initiated by the addition of inhibitor at final concentrations 0.7-fold the K_i, the K_i, 2-fold the K_i, and 10-fold the K_i value for a final incubation volume of 100 μL. After 3, 6, 9, 12, 15, and 20 min, the incubations were stopped by withdrawing 10 μL and freezing the incubation with a dry ice/2-propanol bath. The incubation to determine residual

CYP2A6 functional activity was initiated with vigorous mixing by the addition of an ambient temperature premixed solution (190 μL) containing coumarin (3 μM), 0.1 M Tris buffer (pH 7.5), and the NADPH-generating system as described above to the frozen enzyme solution (10 μL) for a final incubation volume of 0.2 mL. After a 15 min incubation at 37 °C, the incubations were stopped by the addition of 0.75 mL of CH_3CN/CCl_3COOH (80:20, v/v). After centrifugation at 13 000 rpm for 5 min, 200 μL of the supernatant was transferred to a Packard OptiPlate 96 well plate, and the formation of the coumarin metabolite, 7-hydroxycoumarin, was determined fluorometrically using a Wallac Victor^2 1420 Multilabel Counter (Wallac Software Version 2.00 release 9) at excitation and emission wavelengths of 355 and 460 nm, respectively. The inhibitory effect of the 3-heteroaromatic and 3-aliphatic pyridines was assessed from the difference between the sample and a corresponding control that was not preincubated with inhibitor.

Difference Spectra of Test Compounds. For difference spectra measurements, the sample cuvette contained 540 nM CYP2A6dH in 100 μM potassium phosphate buffer (pH 7.4), and the reference cuvette contained only 100 μM potassium phosphate buffer (pH 7.4). The baseline was recorded between 260 and 700 nm. Subsequently, test compound (10 μM in 100% ethanol) was added to both sample and reference cuvettes. The maximal ethanol concentration used was 2%. The difference spectra were obtained after the system reached equilibrium (3 min). All difference spectra were recorded at 25 °C.

Supporting Information Available: A table listing the HPLC retention times and the mobile phase and method for analysis is provided. This material is available free of charge via the Internet at http://pubs.acs.org.

References

(1) U.S. Department of Health and Human Services. *The Health Consequences of involuntary exposure to tobacco smoke: A report of the Surgeon General*; U.S. Department of Health and Human Services, Center for Disease Control and Prevention, Coordinating Center for Health Promotion, National Center for Chronic Disease Prevention and Health Promotion, Office of Smoking and Heatlh: Atlanta, GA, 2006.

(2) Sellers, E. M.; Tyndale, R. F.; Fernandes, L. C. Decreasing smoking behaviour and risk through CYP2A6 inhibition. *Drug Discovery Today* **2003**, *8*, 487−493.

(3) Jorenby, D. Smoking cessation strategies for the 21st Century. *Circulation* **2001**, *104*, e51−e52.

(4) Westmaas, J.; Nath, V.; Brandon, T. Contemporary Smoking Cessation. *Cancer Control J. Moffitt Cancer Cent.* **2000**, *7*, 56−62.

(5) von Weymarn, L. B.; Murphy, S. E. CYP2A13-catalyzed coumarin metabolism: comparison with CYP2A5 and CYP2A6. *Xenobiotica* **2003**, *33*, 73−81.

(6) Cashman J. R.; Park, S. B.; Yang, Z.-C.; Wrighton, S. A.; Jacob, P., III; Benowitz, N. L. Metabolism of nicotine by human liver microsomes: Stereoselective formation of *trans*-nicotine N′-oxide. *Chem. Res. Toxicol.* **1992**, *5*, 639−646.

(7) Benowitz, N. L. Pharmacological Aspects of Cigarette Smoking and Nicotine Addiction. *N. Engl. J. Med.* **1988**, *319*, 1318−1330.

(8) Sellers, E. M.; Zeman M. V.; Kaplan H. L.; Tyndale R. F. Inhibition of cytochrome P4502A6 (CYP2A6) decreases smoking and activation of the procarcinogen 4-(methylnitrosoamino)-1-(3-pyridyl)-1-butanone (NNK) *Clin. Pharmacol. Ther*. **2000**, *67*, 113−118.

(9) Tyndale, R. F.; Sellers, E. M. Variable CYP2A6-mediated nicotine metabolism alters smoking behavior and risk. *Drug Metab. Dispos.* **2001**, *29*, 548−552.

(10) Zhang, W.; Kilicarslam T.; Tyndale R. F.; Sellers E. M. Evaluation of methoxsalen, tranylcylopropylamine and tryptamine as specific and selective CYP2A6 inhibitors in vitro. *Drug Metab. Dispos.* **2001**, *26*, 897−902.

(11) Denton, T. T.; Zhang, X.; Cashman, J. R. 5- and 6-Substituted and unsubstituted 3-heteroaromatic pyridine analogues of nicotine as selective inhibitors of cytochrome P-450 2A6. *J. Med. Chem.* **2004**, *48*, 224−239.

(12) Honkakoski, P.; Negishi, M. The structure, function and regulation of cytochrome P450 2A enzymes. *Drug Metab. Rev.* **1997**, *29*, 977−996.

(13) Dalvie, D. K.; Kalgutkar, A. S.; Khojasteh-Bakht, S. C.; Obach, R. S.; O'Donnell, J. P. Biotransformation reactions of five-membered aromatic heterocyclic rings. *Chem. Res. Toxicol.* **2002**, *15*, 269−299.

(14) Lopez-Garcia, M. P.; Dansette, P. M.; Mansuy D. Thiophene derivatives as new mechanism-based inhibitors of cytochromes P-450: inactivation of yeast-overexpressed human liver cytochrome P-450 2C9 by tienilic acid. *Biochemistry* **1994**, *33*, 166−175.

(15) . Yano, J. K.; Hsu, M. H.; Griffin, K. J.; Stout, C. D.; Johnson, E. F. Structures of human microsomal cytochrome P450 2A6 complexed with coumarin and methoxsalen. *Nat. Struct. Mol. Biol.* **2005**, *12*, 822−823.

(16) Fujita, K.; Kamataki, T. Screening of organosulfur compounds as inhibitors of human CYP2A6. *Drug Metab Dispos.* **2001**, *29*, 983−989.

(17) Nagano, S.; Poulos, T. L. Crystallographic study on the dioxygen complex of wild-type and mutant cytochrome P450cam. Implications for the dioxygen activation mechanism. *J. Biol. Chem.* **2005**, *280*, 31659−31663.

(18) Schlichting, I.; Berendzen, J.; Chu, K.; Stock, A. M.; Maves, S. A.; Benson, D. E.; Sweet, R. M.; Ringe, D.; Petsko, G. A.; Sligar, S. G. The catalytic pathway of cytochrome p450cam at atomic resolution. *Science* **2000**, *287*, 1615−1622.

(19) Hoffman, D.; Hoffmann, I.; El-Bayoumy, K. The less harmful cigarette: A controversial issue. A tribute to Ernst L. Wynder. *Chem. Res. Toxicol.* **2001**, *14*, 767−790.

(20) Wester, M. R.; Stout, C. D.; Johnson, E. F. Purification and crystallization of N-terminally truncated forms of microsomal cytochrome P450 2C5. *Methods Enzymol.* **2002**, *357*, 73−79.

(21) Brunger, A. T.; Adams, P. D.; Clore, G. M.; DeLano, W. L.; Gros, P.; Grosse-Kunstleve, R. W.; Jiang, J. S.; Kuszewski, J.; Nilges, M.; Pannu, N. S.; Read, R. J.; Rice, L. M.; Simonson, T.; Warren, G. L. Crystallography & NMR system: A new software suite for macromolecular structure determination. *Acta Crystallogr., Sect. D: Biol. Crystallogr.* **1998**, *54* (Pt 5), 905−921.

(22) Otwinowski, Z.; Minor, W. Processing of X-ray diffraction data collected in oscillation mode. *Methods Enzymol.* **1997**, *276*, 307−326.

(23) CCP. The CCP4 suite: programs for protein crystallography. *Acta Crystallogr.* **1994**, *D50*, 760−763.

(24) Jones, T. A.; Kjeldgaard, M. Electron-density map interpretation. *Methods Enzymol.* **1997**, *277*, 173−208.

(25) Rieke, R. D.; Kim, S.-H.; Wu, X. Direct preparation of 3-thienyl organometallic reagents: 3-Thienylzinc and 3-thienylmagnesium iodides and 3-thienylmanganese bromides and their coupling reactions. *J. Org. Chem.* **1997**, *62*, 6921−6927.